ChemBioChem

Research Article
doi.org/10.1002/cbic.202300185

Chemistry Europe
European Chemical Societies Publishing

www.chembiochem.org

Facile Production of the *Pseudomonas aeruginosa* Virulence Factor LasB in *Escherichia coli* for Structure-Based Drug Design

Dominik Kolling,[a, b] Jörg Haupenthal,[a] Anna K. H. Hirsch,[a, b] and Jesko Koehnke*[a, c, d]

The human pathogen *Pseudomonas aeruginosa* has a number of virulence factors at its disposal that play crucial roles in the progression of infection. LasB is one of the major virulence factors and exerts its effects through elastolytic and proteolytic activities aimed at dissolving connective tissue and inactivating host defense proteins. LasB is of great interest for the development of novel pathoblockers to temper the virulence, but access has thus far largely been limited to protein isolated from *Pseudomonas* cultures. Here, we describe a new protocol for high-level production of native LasB in *Escherichia coli*. We demonstrate that this facile approach is suitable for the production of mutant, thus far inaccessible LasB variants, and characterize the proteins biochemically and structurally. We expect that easy access to LasB will accelerate the development of inhibitors for this important virulence factor.

Introduction

The Gram-negative ESKAPE pathogen *Pseudomonas aeruginosa* (PA) has a versatile arsenal of insidious virulence factors. They are significantly involved in the infection process and actively drive it. The formation of virulence factors is controlled by bacterial cell–cell communication *via* a tightly regulated quorum-sensing network.[1,2] It also regulates biofilm formation, for which PA is particularly well known.[3] Virulence factors can be divided into those altering the surface structures of the bacterial cell membrane, bacterial cell–cell interactions, and secreted factors.[4] The active secretion of specific factors contributes to host damage during infection. This includes the T3SS effector toxins, which are responsible for the destruction of the host actin skeleton and the zinc-dependent protease LasB, which is responsible for actively driving the infection process.[5,6] The expression of LasB is induced by signaling molecules within the quorum-sensing network during the early phase of PA infection (Figure 1).[7] The proteolytic and elastolytic activity of LasB advances the colonization of the host by PA and interferes with specific defense mechanisms of the infected host. LasB is, for example, able to destroy the structural components of the extracellular matrix of the infected host, such as elastin, collagen, or VE cadherin.[8–10] In addition, defense factors of the human immune system, such as CD4, elafin, and IL-6, are also LasB substrates.[11–13]

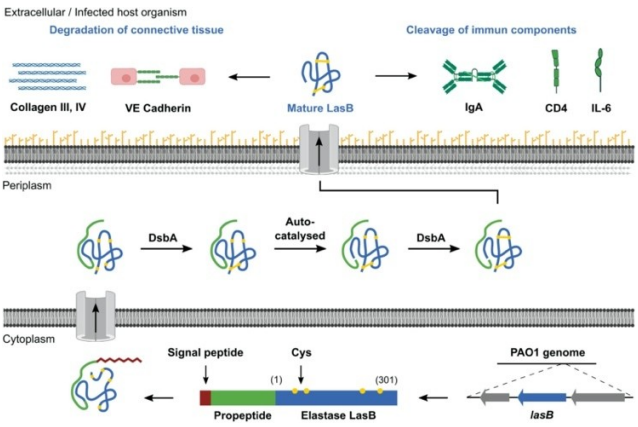

Figure 1. Expression and post-translational processing of LasB in its native host *P. aeruginosa*. Translation of the *lasB* gene is followed by translocation of the encoded pre-propeptide into the periplasm, which is mediated by a signal peptide. The signal peptide is removed, and processing of the enzyme occurs via disulfide bridge assembly using oxidoreductase DsbA. The pre-propeptide remains associated with LasB during this process and serves as both an intramolecular chaperone and elastase inhibitor. After successful folding, LasB is secreted into the extracellular space. Here, components of the extracellular matrix and components of the host immune system are inactivated by cleavage, which allows the infection to proceed largely undisturbed.

[a] *D. Kolling, Dr. J. Haupenthal, Prof. Dr. A. K. H. Hirsch, Prof. Dr. J. Koehnke*
Helmholtz Institute for Pharmaceutical Research Saarland (HIPS)
Helmholtz Centre for Infection Research (HZI)
Campus Building E8.1, 66123 Saarbrücken (Germany)

[b] *D. Kolling, Prof. Dr. A. K. H. Hirsch*
Department of Pharmacy, University of Saarland
Campus Saarbrücken, 66123 Saarbrücken (UK)

[c] *Prof. Dr. J. Koehnke*
School of Chemistry, University of Glasgow
Joseph Black Building
University Avenue, G12 800 Glasgow (UK)

[d] *Prof. Dr. J. Koehnke*
Institute of Food Chemistry, Leibniz University Hannover
Callinstr. 5, 30167 Hannover (Germany)
E-mail: Jesko.Koehnke@lci.uni-hannover.de

Supporting information for this article is available on the WWW under https://doi.org/10.1002/cbic.202300185

This article is part of the Special Collection ChemBioTalents2022. Please see our homepage for more articles in the collection.

LasB was first described almost 60 years ago by Morihara *et al.* and biochemically characterized shortly afterwards. LasB was purified directly from the culture supernatant of PA via a lengthy, multi-step process.[14] The LasB structure was elucidated by X-ray crystallography, and proteolytic and elastolytic activities were demonstrated. Thirty-five years ago the nucleotide sequence of the gene encoding LasB was identified, and first expression experiments based on stable integration of *lasB* into the *Escherichia coli* chromosome were undertaken.[15] While the yield was acceptable, the method has not found broad application and does not allow for the facile expression of different LasB mutants found in clinical isolates. This poses a serious obstacle to attempts to exploit LasB for the development of antivirulence, or pathoblocker, compounds. LasB is a promising, validated target for drug development against serious PA infections, and high-affinity inhibitors with outstanding selectivity over human off-targets have very recently been reported.[16–18] From a medicinal chemistry perspective, extracellular targets are particularly attractive given that the drug candidates do not have to cross the Gram-negative cell membrane to reach their site of action.

LasB is encoded as a pre-proenzyme, which requires several processing steps to become a mature, active protein: First, the unfolded protein is translocated into the periplasm, where two disulfide bridges are formed with the help of oxidoreductases.[19] LasB is then transported across the outer cell membrane into the extracellular space by a secretion apparatus, where LasB and the pre-propeptide complex dissociate.[20,21] A recent attempt to express LasB in *E. coli* strains BL21 and JM109 gave very low yields that could only be detected by immunoblotting.[15,22] As a result, the standard purification procedure for LasB is from the supernatant of PA cultures, which is low-yielding, unpredictable and very time-consuming. Additionally, LasB mutants identified in clinical isolates via sequencing remain largely inaccessible. Everett *et al.* have recently reported that the analysis of LasB activity of clinical isolates is so far only possible in the supernatant and accordingly only in a more complex mixture.[18] For an *in vitro* activity assay, the clinical PA strains would have to be available in the first place and secrete sufficient LasB under laboratory conditions. To address these issues we have developed a high-yielding production protocol for recombinant LasB (LasB*) in *E. coli*, which allows the rapid purification of LasB*. We demonstrate that LasB and LasB* have comparable activities and determined the crystal structure of LasB*. We demonstrate that LasB mutants found in clinical PA isolates are also accessible by our approach and obtained activity and structural data for these mutants.

Results and Discussion

Production of LasB in *E. coli*

We reasoned that the successful past attempt to produce LasB in *E. coli* from a strain that had *lasB* integrated into its genome demonstrated the feasibility of LasB production in *E.* coli. To allow the enzyme's facile production and easy access to LasB mutants we chose a plasmid-based production system. *lasB* was cloned into the pET-26b plasmid, where the native LasB signal peptide was replaced by the signal sequence of PelB and a C-terminal His_6-tag added to LasB. This should allow transport of the pre-proenzyme into the periplasm for further processing and increase the LasB yield. We initially chose *lasB* from the standard laboratory PA strain PAO1 and attempted expression in *E. coli* BL21(DE3) and *E. coli* Rosetta (DE3). However, no soluble protein was produced and the growth of the strains was strongly inhibited. As the expression of LasB appeared to be toxic to the respective strains, the strain *E. coli* Lemo 21, optimized for the production of proteins toxic to *E. coli*, was tested. During subsequent cultivation, successful expression of soluble $LasB^*_{PAO1}$ in *E. coli* was detected by SDS-PAGE (Figure S1 in the Supporting Information). Subsequent determination of the intact protein mass by LC-MS confirmed the identity of $LasB^*_{PAO1}$.

As reported in previous studies, the pre-propeptide plays a crucial role in the expression and subsequent processing of LasB: The construct pET-26b-$LasB^*_{PAO1\Delta IMC}$ was designed, in which the signal peptide PelB was fused directly to the sequence of mature $LasB^*_{PAO1}$. When this construct was expressed as described above, no LasB expression could be detected by SDS-PAGE.

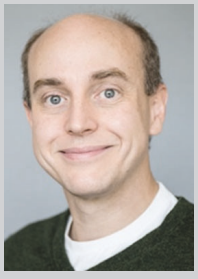

Jesko Köhnke studied biochemistry at Leibniz University Hannover (LUH), Germany, graduating in 2005. After a PhD at Columbia University, USA, under the supervision of Prof. Lawrence Shapiro, he joined the group of Prof. James Naismith at the University of St Andrews, UK, as a postdoctoral researcher in 2010. From 2015–2020 he was a junior group leader at the Helmholtz Institute for Pharmaceutical Research Saarland, Germany. In 2018 he was also appointed an associated Junior Professor at Saarland University. He moved to the University of Glasgow, UK, as a Reader in 2020 and was promoted to Professor in 2022. In 2023 he returned to LUH as the managing director of the Institute of Food Chemistry. His work focuses on the structural biology and biochemistry of natural product biosynthesis.

Dominik Kolling studied Pharmacy at the University of Saarland, Germany. He pursued his MSc under the Supervision of Prof. Dr. Andriy Luzhetskyy in the field of pharmaceutical biotechnology and natural product discovery. In 2021, he joined the group of Prof. Dr. Jesko Köhnke in collaboration with Prof. Dr. Anna K. H. Hirsch at the Helmholtz Institute for Pharmaceutical Research Saarland, Germany. His work focuses on structural biology with application in drug discovery and drug design as well as proteins involved in natural product biosynthesis.

Mutation of the catalytically essential amino acid His223 (zinc-binding) to Tyr (pET-26b-LasB*$_{PAO1H223Y}$) resulted in the accumulation of the fusion protein prepro-LasB, which supports the notion of autocatalytic processing of LasB (Figure S2A).[16]

To determine if LasB expression in *E. coli* could provide the yields necessary for biological testing in the context of the development of LasB inhibitors, we attempted large-scale purification. Here, knowledge that LasB processing was autocatalytic proved essential: When the immobilized metal affinity chromatography (IMAC) column was loaded at room temperature and washed with lysis buffer, LasB*$_{PAO1}$ eluted before a higher imidazole concentration was applied (Figure S3). Analysis of this protein fraction by SDS-PAGE and intact protein mass spectrometry confirmed the presence of LasB*$_{PAO1}$ without a His_6-tag. The enzyme thus released itself from the column during purification in an autocatalytic process. Based on analysis of the intact mass of purified LasB*$_{PAO1}$, we could identify a self-cleavage site after Ser299. (Figure 2)

This unusual purification method had two advantages: First, enzyme activity was confirmed during purification. Second, it can be assumed that the pre-elution peak has a higher purity because only LasB*$_{PAO1}$ selectively removes itself from the column. Interestingly, this effect could only be observed when sufficiently high density of LasB*$_{PAO1}$ was achieved on the resin. This indicates that cleavage occurs *in trans*, a notion supported by the distance between cleavage-site and active-site observed in LasB crystal structures, which is too large to allow cleavage *in cis*.

After final size-exclusion chromatography, impurities were observed on the SDS-PAGE gel. We suspected that these lower molecular weight bands were proteolysis products of LasB. Analysis of three gel bands by tryptic digest, followed by MS/MS[2] analysis, confirmed this suspicion (Figure S7). To determine the conditions under which LasB degrades, analytical size-exclusion chromatography was performed, and LasB was incubated at 37 °C with and without EDTA (Figure S8). Little degradation was observed, which prompted us to investigate the influence of SDS, which is present in gel loading buffer. Analytical size-exclusion chromatography demonstrates that addition of SDS, particularly in combination with boiling, leads to rapid LasB degradation (Figure S8). Because gel samples are usually of higher concentrations and not all LasB molecules would unfold instantly, it seems that LasB can rapidly digest itself, making SDS-PAGE samples appear less pure than they actually are.

To further increase the yield of LasB, the purification was optimized by loading the column at 4 °C. This prevented LasB self-cleavage and thus release from the column. After loading and extensive washes, the column was disconnected and incubated at room temperature to allow autocatalytic self-digestion to occur more quickly and quantitatively. Through the described optimization, a final yield of 15 mg active LasB*$_{PAO1}$ per liter of culture could be obtained.

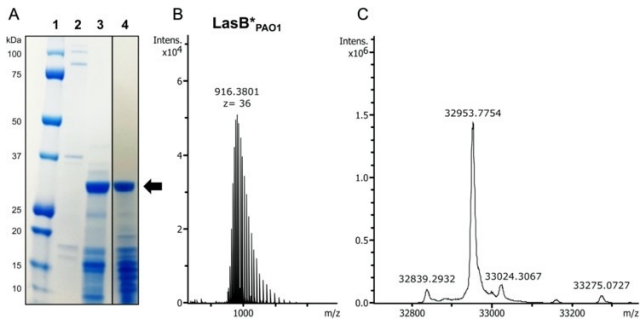

Figure 2. A) SDS-PAGE analysis of LasB* expression in *E. coli* Lemo21. Molecular weight maker (lane 1), uninduced control of *E. coli* Lemo21 harboring the plasmid pET-26b-LasB*$_{PAO1}$ (lane 2), and affinity-purified and recombinantly expressed LasB*$_{PAO1}$ in *E. coli* Lemo21 (lane 3), LasB*$_{PAO1}$ after size-exclusion chromatography (lane 4). Lane 4 was part of the same gel as lanes 1–3, samples in between were removed for clarity. B) ESI-MS spectrum of LasB*$_{PAO1}$ purified from *E. coli.* C) Deconvoluted ESI-MS spectrum of the purified LasB*$_{PAO1}$. The major peak at *m/z* 32953 Da correlates with the mass of LasB*$_{PAO1}$, where both the His tag and TEV site were autocatalytically removed. The LasB cleavage site could be identified and is located after LasB*$_{PAO1}$ Ser299, removing the last two amino acid residues Ala300 and Leu301 from the C terminus. The additional, minor peaks correspond to alternative cleavage products (Table S2).

Analysis of LasB sequences from clinical isolates

As mentioned above, LasB is a promising target for the treatment of PA infections. Targeted inhibition of bacterial virulence factors by small molecules is the concept of pathoblockers.[23] Treatment with traditional antibiotics usually kills bacteria, which increases selection pressure and promotes the development of resistance.[24] Pathoblockers on the other hand were developed to render bacteria harmless by inhibiting host-damaging virulence factors. This is expected to result in a lower mutation rate for the corresponding target, which should ensure the persistent effect of pathoblockers.[25]

To determine the diversity of LasB sequences found in clinical isolates of PA, we used the public database for molecular typing and microbial genome diversity (PubMLST), where the genomic information of 2863 PA strains was available.[26] The LasB amino acid sequences of the two standard laboratory strains, PAO1 and PA14, from which LasB had already been purified, were used as inputs. Subsequent analysis showed that 72% of all LasB sequences were identical to those of either PAO1 or PA14 (Figure 3). The remaining 28% were LasB variants

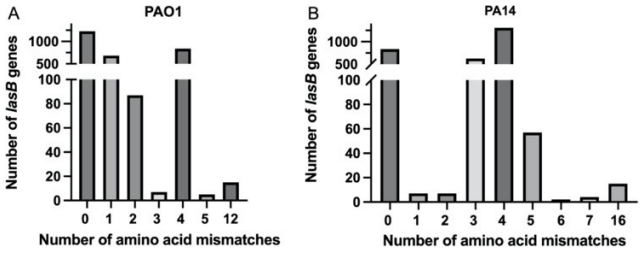

Figure 3. Results of PubMLST blast analysis with the LasB sequence from A) PAO1 or B) PA14 as input. For sequence alignment, 72% of all LasB entries from the database showed a 100% match to the LasB sequences of either PA14 or PAO1. However, the LasB sequences of the two strains differed by 4 amino acids. The remaining 28% of the database entries correlate with LasB sequences with a different number of mismatches. Up to 12 (PAO1) and 16 (PA14) mismatches can be observed.

with various numbers of mutations, ranging from one mismatch to 16 in rarer cases (0.5 %). With regard to the validation of LasB as a drug target, biochemical characterization of these currently rare LasB variants is of particular interest. Yet cultivation of the corresponding strains and purification of LasB from their supernatant is impossible, because the clinical isolates are usually used for sequencing and not kept for later use. We hoped that our newly established LasB production procedure would allow us to produce and test one of the rare variants.

We thus selected the LasB with the most distant sequence homology to the already well-characterized LasBs from PA14 and PAO1 (16 and 12 mismatches, respectively) from the database. This LasB variant is expressed by strain PA7 (LasB*$_{PA7}$) and a few other representatives. In addition, a non-natural LasB variant was constructed by introducing the unique Met120Val mutation found in strain AZPAE14816 into the PA7 LasB sequence (LasB*$_{Artif}$).

Production and characterization of LasB variants

The selected LasB variants were expressed in *E. coli* and purified as described above. In a FRET-based *in vitro* assay, the proteolytic activity of LasB$_{PA14}$, purified from the culture supernatant of PA14 (LasB$_{PA14}$), was compared with that of LasB*$_{PAO1}$, LasB*$_{PA7}$, and LasB*$_{Artif}$ produced in *E. coli*.

Analysis of these data showed that the activities of LasB$_{PA14}$ and recombinant LasB*$_{PAO1}$ were almost identical, whereas that of LasB*$_{PA7}$ slightly increased. However, mutation Met120Val in LasB*$_{Artif}$ led to a significant decrease in proteolytic activity.

To further illustrate that recombinantly produced LasB is suitable for drug design endeavors, we used all four proteins in a FRET-based *in vitro* inhibition assay with a known LasB inhibitor (Figure 4).

This inhibitor is a previously reported prodrug-like compound, in which a thiocarbamate motif is rapidly hydrolyzed in the buffer to the free thiol.[27] LasB inhibition is achieved by the free thiol acting as a zinc-binding group to complex the catalytically active metal cation in the substrate-binding pocket (Figure S9). The compound had highly similar IC$_{50}$ values for all three proteins, LasB*$_{PA14}$, LasB*$_{PAO1}$, and LasB*$_{PA7}$. Surprisingly, LasB*$_{Artif}$, which was less active in the FRET assay, could be inhibited more readily and thus displayed a lower IC$_{50}$ value.

X-ray crystallography

A very important aspect of medicinal chemistry programs for any target is crystallizability of the target protein. While we were satisfied that LasB*$_{PA01}$ and LasB purified from PA supernatant had very similar activities and inhibition profiles, we also wanted to use this opportunity to demonstrate that the recombinant LasB* was structurally identical to LasB from PA and could be readily crystallized. To this end, we crystallized LasB*$_{PA01,}$ LasB*$_{PA7}$ and LasB*$_{Artif}$ and determined their structures to 1.1, 1.5, and 0.9 Å resolution, respectively. All data collection and refinement statistics can be found in Table S3. The overall

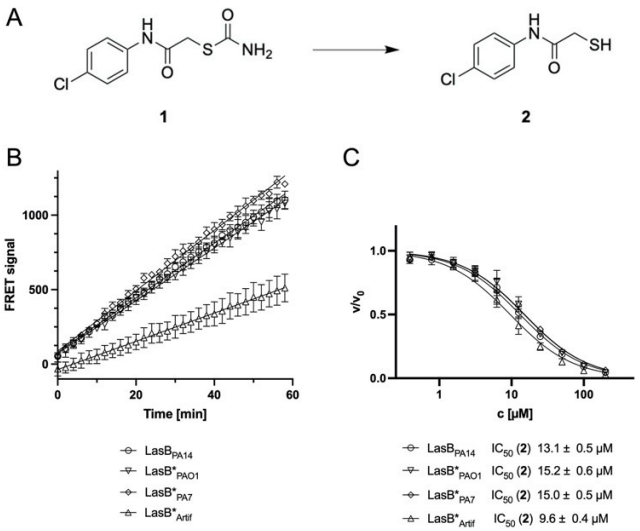

Figure 4. A) Hydrolysis of the thiocarbamate **1** to the active thiol-based LasB inhibitor **2** in aqueous buffer. B) Comparison of the activity of LasB variants purified from *E. coli* with the activity of LasB purified from PA14. The activity of LasB*$_{PAO1}$ expressed in *E. coli* is comparable to that of LasB purified from the native host strain PA14. The proteolytic activity of LasB*$_{PA7}$ was slightly higher than that of the other variants. The activity of LasB*$_{Artif}$ is approximately half that of the other proteins. C) In vitro FRET inhibition assay to determine the IC$_{50}$ of compound **2** against different LasB variants. The IC$_{50}$ for the LasB variants LasB*$_{PA14}$, LasB*$_{PAO1}$, and LasB*$_{PA7}$ were very similar, but the IC$_{50}$ for LasB*$_{Artif}$ was lower than that of the other LasB variants.

structures were very similar with pairwise C$_\alpha$ rmsd values below 0.6 Å and differed mainly in the more flexible loop regions of the protein (Figure 5A). As differences were found in the activity of the LasB variants, it is particularly interesting to compare the structure of the active site in a superposition with LasB*$_{PAO1}$. Here, we observed that in both LasB*$_{PA7}$ and LasB*$_{Artif}$, the antiparallel β-sheet adjacent to the active-site zinc cation had shifted closer to the metal ion (Figure 5B). When comparing the protein surfaces, it becomes clear that the substrate binding pocket is increasingly narrowed in LasB*$_{PA7}$ and LasB*$_{Artif}$ compared to LasB*$_{PAO1}$ (Figures S11 and S12). Overall none of the mutations occur directly at the active or allosteric site, which we view as a positive, because there do not appear to be resistant versions of LasB in circulation yet (Figure S13).

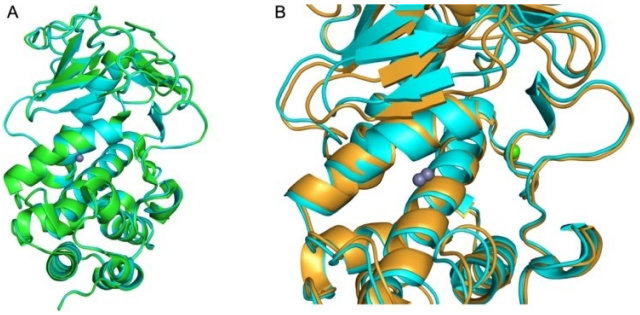

Figure 5. A) Superposition of cartoon representations of LasB*$_{PAO1}$ (cyan) and LasB purified from PA supernatant (green, PDB ID: 1EZM). B) Superposition of cartoon representations of LasB*$_{PA7}$ (orange) and LasB*$_{PAO1}$ (cyan) zoomed in on the antiparallel β-sheet in the active site.

As LasB*$_{Artif}$ contains the extremely rare mutation Met120Val, we suspected that the conformational change of LasB restricts substrate binding. LasB undergoes a conformational shift from open to closed conformation upon substrate binding, and for LasB*$_{Artif}$ we observe a protein conformation that appears to be en route to the closed, substrate-bound state, even though neither substrate nor inhibitor are bound at the active-site. This might explain the diminished proteolytic activity of this mutant.

Conclusions

Currently, the need for new therapeutic approaches and novel antibiotics against the pathogen *P. aeruginosa* is crucial, especially against the background of the rapid development of resistance. Targeted inhibition of virulence factors with patho-blockers renders the pathogen harmless while reducing the selection pressure to evolve resistant mutants.

Here, we have demonstrated that the virulence factor LasB can readily be produced in *E. coli* to meet the increased demand for drug design and the optimization of LasB inhibitors. Compared to the previous purification procedure from the culture supernatant of PA, not only are larger quantities produced, but also more reproducible yields are achieved. LasB obtained by affinity chromatography was also tested for its use in structure-based drug design approaches. Crystal structures with excellent resolution, which are particularly suitable for structure-based design in drug discovery, were obtained readily from the recombinantly produced proteins. In this context, high-throughput compound screening is also aided by the availability of LasB in sufficient quantities. Further drug optimization can be performed quickly and effectively based on the co-crystal structures.

In addition, the system presented here is ideally suited for studies of the effects of LasB mutations found in clinical isolates of PA, for example on substrate profiles or susceptibility to inhibitors under development. We hope that the ready access to LasB variants, even those with rare mutations, will accelerate drug-discovery programs for this important target.

Experimental Section

Cloning and expression of LasB: The synthetic codon-optimized genes for LasB*$_{PAO1}$, LasB*$_{PA7}$, and LasB*$_{Artif}$ were ordered already cloned in the expression vector pET-26b(+) from the commercial manufacturer BioCat, Heidelberg, Germany. The construct pET-26b-LasB* with a C-terminal His-tag and TEV protease site (ENLYFGQ) was transformed into electrocompetent *E. coli* Lemo 21 and plated on agar plates containing the selection antibiotics kanamycin (50 μg mL^{-1}) and chloramphenicol (25 μg mL^{-1}). The constructs for the expression of LasB*$_{PAO1\Delta IMC}$ and inactive LasB*$_{PAO1H223Y}$ in pET-26b(+) were prepared by Gibson assembly. Primers and expressed protein sequences can be found in Table S3, and the synthetic construct pET-26b-LasB*$_{PAO1}$ was used as a template for PCR. The PCR products were purified for both the vector and insert using agarose gel electrophoresis and the QIAquick Gel Extraction Kit from Qiagen. For subsequent homologous recombination by Gibson assembly, a standard protocol was used. Positive clones of *E. coli* HS996 were selected, plasmid DNA was isolated, and the sequence of the final construct was confirmed using Sanger sequencing. The plasmids were then transformed into the expression strain *E. coli* Lemo 21 as mentioned above. A single colony was used to inoculate the preculture in LB medium supplemented with the appropriate antibiotics, and the flasks were incubated overnight at 37 °C with shaking at 180 rpm. This culture was used to inoculate the main LB culture on the following day. The culture was incubated at 37 °C and 180 rpm until an OD_{600} of 0.8 was reached. Protein expression was then induced with 1 mM IPTG and the culture was incubated at 18 °C and 180 rpm overnight. Cells were harvested the following day by centrifugation at 12 800 *g* at 4 °C for 15 min. The cell pellet was flash-frozen in liquid nitrogen and stored at −80 °C until further use.

Purification of LasB*$_{PAO1}$, LasB*$_{PA7}$ and LasB*$_{Artif}$: Purification of LasB* and all variants was performed using lysis buffer A (50 mM Tris, pH 8.0, 150 mM NaCl, 10% glycerol, and 20 mM imidazole) supplemented with DNase (0.4 mg/g wet cell pellet). The bacterial cell pellet was resuspended in lysis buffer and lysed by passing it through a cell disruptor twice at 24.5 kPSI and cooling at 4 °C. Subsequently, cell debris was removed by centrifugation at 35 000 *g* at 4 °C for 30 min. The lysate was then filtered through a filter with a pore size of 0.45 μm and loaded onto a HisTrap HP 5 mL column pre-equilibrated with buffer A using an ÄKTA pure at 4 °C. The column was then washed with five CV of buffer A, disconnected from the ÄKTA, and incubated at RT for 1.5 h. The LasB-containing fractions of the pre-elution with buffer A were collected and concentrated using a 10 kDa cut-off Amicon concentrator. The protein sample was then applied to a Superdex S200 16/600 column pre-equilibrated with final storage buffer C (10 mM Tris pH 8.0, 2 mM $CaCl_2$). Protein fractions containing LasB were pooled and concentrated to 5 mg mL^{-1}. Protein concentrations were determined by the specific absorption coefficient at A280 using a Nanodrop, and purity was checked by SDS-PAGE.

Purification of LasB$_{PA14}$: Cultivation of PA14, collection of culture supernatant, and purification were performed as previously described.[27]

Analytical size-exclusion chromatography: Protein purity and stability were analyzed using a Superose™ 6 10/300 gel filtration column preequilibrated with storage buffer C (10 mM Tris pH 8.0, 2 mM $CaCl_2$). Purified LasB*$_{PAO1}$ (150 μL, 5.2 mg mL^{-1}) was incubated for 1 h and 6 h at 37 °C and a total amount of 780 μg was loaded on onto the column. The LasB stability was further assayed by gel filtration in the presence of 6 mM ETDA under the same incubation conditions and subsequently after the addition of 1% SDS with and without boiling the sample for 5 min at 95 °C.

Intact protein mass spectrometry: LC–MS measurements to determine the intact protein mass were performed using a Dionex Ultimate 3000 RSLC system equipped with an Aeris Widepore XB-c8 (150×2.1 mm, 3.6 μm particle diameter(dp)) column (Penomenex, USA). The LC was coupled to a maXis 4G high-resolution time-of-flight (HR-ToF) mass spectrometer (Bruker Daltonic) using an Apollo electrospray ionization (ESI) source. Separation of 5 μL protein sample on the LC was achieved by a linear gradient from solvent A (H_2O plus 0.1% formic acid) to solvent B (acetonitrile plus 0.1% formic acid) as follows: 0–0.5 min (2%), 0.5–10.0 min (2–75%), 10.0–13.0 min (75%), 13.0–18.0 min (2%). The following conditions were used for mass spectrometry: capillary voltage 4000 V, temperature 200 °C, dry gas flow rate 5 L min^{-1} and nebulizer 14.5 psi. Data were recorded in a mass range of 150–2500 *m/z*. Sodium formate clusters were used for calibration of the maXis 4G spectrometer before every injection to avoid mass drift.

In vitro inhibition assay: FRET-based activity and inhibition assays were performed as previously described.[27] Briefly, the assay was

performed in a black 384-well microtiter plate (Greiner BioOne, Kremsmünster, Austria) using a CLARIOstar microplate reader. The excitation wavelength was 340 ± 15 nm and the emission at 415 ± 20 nm was measured for 60 min at 37 °C. The assay was performed in a final volume of 50 μL assay buffer (50 mM Tris, pH 7.2, 2.5 mM $CaCl_2$, 0.075% Pluronic F-127, 5% DMSO). The LasB concentration was 0.3 nM and that of the FRET substrate (2-aminobenzoyl-Ala-Gly-Leu-Ala-4-nitrobenzylamide, Peptides International, Louisville, KY, USA) was 150 μM. Purified $LasB_{PA14}$ and LasB* variants expressed in *E. coli* were used in the assay at a final concentration of 0.13 nM. The purity of the protein samples was analyzed by SDS-PAGE. The experiments were performed in duplicate and repeated three times. Analysis of the assay results was performed as previously described, and the results were visualized using GraphPad Prism X.

X-ray crystallography: Initial screening experiments for $LasB^*_{PAO1}$, $LasB^*_{PA7}$, and $LasB^*_{Artif}$ were performed using a protein concentration of ~5 mg mL^{-1} and commercially available crystallization screens (NeXtal). The screens were carried out on sitting-drop SwissSCI plates using a Gryphon crystallization robot. Crystals for all LasB* variants were observed after an incubation time of approximately one month at 277 K. For $LasB^*_{PAO1}$, the crystals appeared in a well solution of 0.2 M magnesium formate and 20% (*w*/*v*) PEG 3350 at a protein concentration of 5.1 mg mL^{-1}. Crystals for the variant $LasB^*_{PA7}$ were grown at a protein concentration of 5.2 mg mL^{-1} in a well solution of 0.2 M magnesium acetate, 0.1 M sodium cacodylate pH 6.5 and 30% (*v*/*v*) MPD. Protein crystals for $LasB^*_{Artif}$ were observed at a slightly higher protein concentration of 5.7 mg mL^{-1} in a well solution of 0.05 M potassium chloride, 0.01 M magnesium chloride and 15% (*w*/*v*) PEG 6000. The obtained crystals were cryoprotected with 32% glycerol before flash-freezing in a cryo-loop. The datasets for all crystals were collected at the ESRF beamlines at 100 K. A high-resolution dataset for $LasB^*_{PAO1}$ was collected at Beamline ID30B. Datasets for the other proteins $LasB^*_{PA7}$ and $LasB^*_{Artif}$ were collected at Beamline ID23-1. The structures were determined by molecular replacement using Phenix.[28] The crystal structure of $LasB_{PAO1}$ (PDB ID: 1EZM) was used as the search model. The structures were rebuilt manually in COOT and further refined using Phenix.refine.[29,30]

Acknowledgements

We acknowledge the use of the ESRF beamlines ID30B and ID23-1. We thank Simone Amann for the PA cultivation and supernatant preparation and Timo Risch for conducting the protein LC–MS measurements. We thank Dr. Andreas Kany for kindly providing compound **1**. We thank Dr. Sally Shirran from the mass spectrometry and proteomics facility at St. Andrews University for conducting the tryptic LasB digesting and MS/MS^2 measurements. Figure 1 and the table of contents graphic were prepared by using BioRender.com (2023). This work was supported by an ANR/BMBF grant (LasBAntiv, 16GW0346) to A.K.H.H. and J.K. Open Access funding enabled and organized by Projekt DEAL.

Conflict of Interests

The authors declare no conflict of interest.

Data Availability Statement

The data that support the findings of this study are available from the corresponding author upon reasonable request.

Keywords: anti-infective agents · LasB · pathoblockers · virulence factors

[1] T. G. Sana, R. Lomas, M. R. Gimenez, A. Laubier, C. Soscia, C. Chauvet, A. Conesa, R. Voulhoux, B. Ize, S. Bleves, *J. Bacteriol.* **2019**, *201*, DOI: 10.1128/jb.00362-19.
[2] J. Lee, L. Zhang, *Protein Cell* **2015**, *6*, 26–41.
[3] M. T. T. Thi, D. Wibowo, B. H. A. Rehm, *Int. J. Mol. Sci.* **2020**, *21*, 8671.
[4] A. Grace, R. Sahu, D. R. Owen, V. A. Dennis, *Front. Microbiol.* **2022**, *13*, 1023523.
[5] G. Horna, J. Ruiz, *Microbiol. Res.* **2021**, *246*, 126719.
[6] M. J. Everett, D. T. Davies, *Drug Discovery Today* **2021**, 2108–2123, DOI 10.1016/j.drudis.2021.02.026.
[7] L. R. Hoffman, H. D. Kulasekara, J. Emerson, L. S. Houston, J. L. Burns, B. W. Ramsey, S. I. Miller, *J. Cystic Fibrosis* **2009**, *8*, 66–70.
[8] N. Beaufort, E. Corvazier, S. Mlanaoindrou, S. de Bentzmann, D. Pidard, *PLoS One* **2013**, *8*, e75708.
[9] C. Wolz, E. Hellstern, M. Haug, D. R. Galloway, M. L. Vasil, G. Döring, *Mol. Microbiol.* **1991**, *5*, 2125–2131.
[10] T. Nagano, J. L. Hao, M. Nakamura, N. Kumagai, M. Abe, T. Nakazawa, T. Nishida, *Invest. Ophthalmol. Visual Sci.* **2001**, *42*, 1247–53.
[11] N. Guyot, G. Bergsson, M. W. Butler, C. M. Greene, S. Weldon, E. Kessler, R. L. Levine, S. J. O'Neill, C. C. Taggart, N. G. McElvaney, *Biol. Chem.* **2010**, *391*, 705–716.
[12] V. Saint-Criq, B. Villeret, F. Bastaert, S. Kheir, A. Hatton, A. Cazes, Z. Xing, I. Sermet-Gaudelus, I. Garcia-Verdugo, A. Edelman, J.-M. Sallenave, *Thorax* **2018**, *73*, 49.
[13] B. K. Pedersen, A. Kharazmi, T. G. Theander, N. Odum, V. Andersen, K. Bendtzen, *Scand. J. Immunol.* **1987**, *26*, 91–94.
[14] K. Morihara, H. Tsuzuki, T. Oka, H. Inoue, M. Ebata, *J. Biol. Chem.* **1965**, *240*, 3295–3304.
[15] R. A. Bever, B. H. Iglewski, *J. Bacteriol.* **1988**, *170*, 4309–4314.
[16] V. Camberlein, G. Jézéquel, J. Haupenthal, A. K. H. Hirsch, *Antibiotics* **2022**, *11*, 1060.
[17] J. Konstantinovic, A. M. Kany, A. Alhayek, A. S. Abdelsamie, A. Sikandar, K. Voos, Y. Yao, A. Andreas, R. Shafiei, B. Loretz, E. Schönauer, R. Bals, H. Brandstetter, R. W. Hartmann, C. Ducho, C.-M. Lehr, C. Beisswenger, R. Müller, K. Rox, J. Haupenthal, A. K. H. Hirsch, *ChemRxiv preprint* **2023**, DOI 10.26434/chemrxiv-2023-bszcb.
[18] M. J. Everett, D. T. Davies, S. Leiris, N. Sprynski, A. Llanos, J. M. Castandet, C. Lozano, C. N. LaRock, D. L. LaRock, G. Corsica, J.-D. Docquier, T. D. Pallin, A. Cridland, T. Blench, M. Zalacain, M. Lemonnier, *ACS Infect. Dis.* **2023**, *9*, 270–282.
[19] P. Braun, C. Ockhuijsen, E. Eppens, M. Koster, W. Bitter, J. Tommassen, *J. Biol. Chem.* **2001**, *276*, 26030–26035.
[20] K. S. McIver, E. Kessler, J. C. Olson, D. E. Ohman, *Mol. Microbiol.* **1995**, *18*, 877–889.
[21] E. Kessler, M. Safrin, *J. Biol. Chem.* **1994**, *269*, 22726–22731.
[22] O. O. Odunuga, O. A. Adekoya, I. Sylte, *Protein Expression Purif.* **2015**, *113*, 79–84.
[23] K. Voos, E. Schönauer, A. Alhayek, J. Haupenthal, A. Andreas, R. Müller, R. W. Hartmann, H. Brandstetter, A. K. H. Hirsch, C. Ducho, *ChemMedChem* **2021**, *16*, 1257–1267.
[24] A. E. Clatworthy, E. Pierson, D. T. Hung, *Nat. Chem. Biol.* **2007**, *3*, 541–548.
[25] R. C. Allen, R. Popat, S. P. Diggle, S. P. Brown, *Nat. Rev. Microbiol.* **2014**, *12*, 300–308.
[26] K. A. Jolley, J. E. Bray, M. C. J. Maiden, *Wellcome Open Res.* **2018**, *3*, 124.
[27] A. M. Kany, A. Sikandar, J. Haupenthal, S. Yahiaoui, C. K. Maurer, E. Proschak, J. Köhnke, R. W. Hartmann, *ACS Infect. Dis.* **2018**, *4*, 988–997.
[28] P. D. Adams, P. V. Afonine, G. Bunkóczi, V. B. Chen, I. W. Davis, N. Echols, J. J. Headd, L.-W. Hung, G. J. Kapral, R. W. Grosse-Kunstleve, A. J. McCoy, N. W. Moriarty, R. Oeffner, R. J. Read, D. C. Richardson, J. S. Richardson, T. C. Terwilliger, P. H. Zwart, *Acta Crystallogr. Sect. D* **2010**, *66*, 213–221.
[29] A. J. McCoy, R. W. Grosse-Kunstleve, P. D. Adams, M. D. Winn, L. C. Storoni, R. J. Read, *J. Appl. Crystallogr.* **2007**, *40*, 658–674.

[30] P. Emsley, B. Lohkamp, W. G. Scott, K. Cowtan, *Acta Crystallogr. Sect. D* **2010**, *66*, 486–501.
[31] F. Madeira, Y. mi Park, J. Lee, N. Buso, T. Gur, N. Madhusoodanan, P. Basutkar, A. R. N. Tivey, S. C. Potter, R. D. Finn, R. Lopez, *Nucleic Acids Res.* **2019**, *47*, W636–W641.

Manuscript received: March 8, 2023
Revised manuscript received: May 14, 2023
Accepted manuscript online: May 17, 2023
Version of record online: July 31, 2023